A chemically powered unidirectional rotary molecular motor based on a palladium redox cycle

Collins, Beatrice S. L.; Kistemaker, Jos C. M.; Otten, Edwin; Feringa, Ben L.

Published in:
Nature Chemistry

DOI:
10.1038/NCHEM.2543

ARTICLES
PUBLISHED ONLINE: 6 JUNE 2016 | DOI: 10.1038/NCHEM.2543
nature chemistry

A chemically powered unidirectional rotary molecular motor based on a palladium redox cycle

Beatrice S. L. Collins, Jos C. M. Kistemaker, Edwin Otten and Ben L. Feringa*

The conversion of chemical energy to drive directional motion at the molecular level allows biological systems, ranging from subcellular components to whole organisms, to perform a myriad of dynamic functions and respond to changes in the environment. Directional movement has been demonstrated in artificial molecular systems, but the fundamental motif of unidirectional rotary motion along a single-bond rotary axle induced by metal-catalysed transformation of chemical fuels has not been realized, and the challenge is to couple the metal-centred redox processes to stepwise changes in conformation to arrive at a full unidirectional rotary cycle. Here, we present the design of an organopalladium-based motor and the experimental demonstration of a 360° unidirectional rotary cycle using simple chemical fuels. Exploiting fundamental reactivity principles in organometallic chemistry enables control of directional rotation and offers the potential of harnessing the wealth of opportunities offered by transition-metal-based catalytic conversions to drive motion and dynamic functions.

While facing the challenge of designing autonomous rotary molecular motors that will ultimately power our future nanoscale machinery, it has become increasingly clear that achieving directional rotary motion through the conversion of a chemical fuel, as is observed in biological systems, remains a formidable task. Although directional motion has been realized in a variety of molecular systems[1–6] (including light-driven directional rotary motion around an overcrowded alkene[7,8], unidirectional rotation in mechanically interlocked molecular systems[9,10] and the directional linear movement in rotaxanes[11,12] and of walkers along tracks[13,14]), arguably one of the most fundamental motifs is the unidirectional rotary motion of one component of a molecule with respect to another about a single C–C bond, as studied by both Kelly and co-workers[15] and our group[16]. In the design presented here, using metal-based chemical transformations, we take as the basis of a rotary motor a simple biaryl molecule with three *ortho* functional groups designated A, B and C, and four distinct steps, as depicted in Fig. 1a.

There are two fundamental requirements for achieving the unidirectional rotation of one aryl group with respect to the other about the single C–C bond. For clockwise rotation, for example, we must be able to control the following: (1) which two *ortho* substituents pass one another (B and A must first cross (station II), followed by C and A (station IV)) and (2) the direction of this crossing (when B crosses A it must do so through a clockwise rotation of the upper ring with respect to the lower aryl ring). The biaryl in station I is atropisomeric to that in station III, where the chirality over the biaryl axis is inverted. If the *ortho* functional group A possesses some further element of chirality, say central chirality (indicated by an asterisk in Fig. 1a), then stations I and III become atropdiastereomeric and possess different energies. Although stations I and III are configurationally stable with respect to the biaryl axis, because rotation about the biaryl bond is restricted by the steric interactions of the *ortho* substituents A, B and C, a conformational change by biaryl rotation allows A and B or A and C to come into close proximity. The barrier to atropisomerization in biaryls can be considerably reduced through the formation of bridges between the *ortho* substituents in the upper and lower rings, as pioneered by Bringmann and co-workers[17,18] and explored in a number of elegant strategies for the asymmetric synthesis of enantioenriched axially chiral biaryls[19–22].

As shown in Fig. 1a, we postulate that, by the addition of a metal M^1 that exhibits selective binding for *ortho* groups A and B, we could facilitate the movement of the biaryl from station I into station III, via the configurationally labile biaryl–metal complexes in station II. The equilibrium established in station II will result in a predominance of the more stable atropdiastereomeric complex, and decomplexation of M^1 in step 2 leads to station III and a complete inversion of axial chirality. Station III cannot be returned directly to station I, as the biaryl is again 'locked' in this axial conformation. The addition of a second, different metal M^2 then gives selective complexation of A and C, leading to station IV, in which the biaryl axis again becomes configurationally labile upon formation of the metal bridge, and the diastereomeric relationship between the central chirality at A and the chirality over the biaryl axis leads to inversion of the axial stereochemistry. Following decomplexation of M^2, the system is returned to station I and a full 360° unidirectional rotation has occurred. There are three key factors that govern the system: (1) selective binding of the two different pairs of *ortho* functional groups with the two different metals; (2) lowering of the barrier to biaryl rotation on complexation of the metal; and (3) transfer of chiral information across the metal centre between the central chirality at A and the biaryl axis, leading to diastereomeric complexes with sufficient energy differences to ensure selective unidirectional rotation of the upper aryl ring.

Driven by our long-standing interest in the development of autonomous unidirectional molecular motors, we envisioned that the decomplexation of M^1 described in step 2 could be coupled with the transformation of M^1 into M^2. This seemingly simple extension of the described system would represent a major advance in the field of unidirectional molecular motors: if M^1 can be transformed into M^2, then step 3 should occur spontaneously, underpinning an autonomous rotation. This autonomy would be rendered complete if M^2 can also be transformed back into M^1 during step 4. Drawing on one of the most integral aspects of

Centre for Systems Chemistry, Stratingh Institute for Chemistry and Zernike Institute for Advanced Materials, Faculty of Mathematics and Natural Sciences, University of Groningen, Nijenborgh 4, 9747 AG Groningen, The Netherlands. *e-mail: b.l.feringa@rug.nl

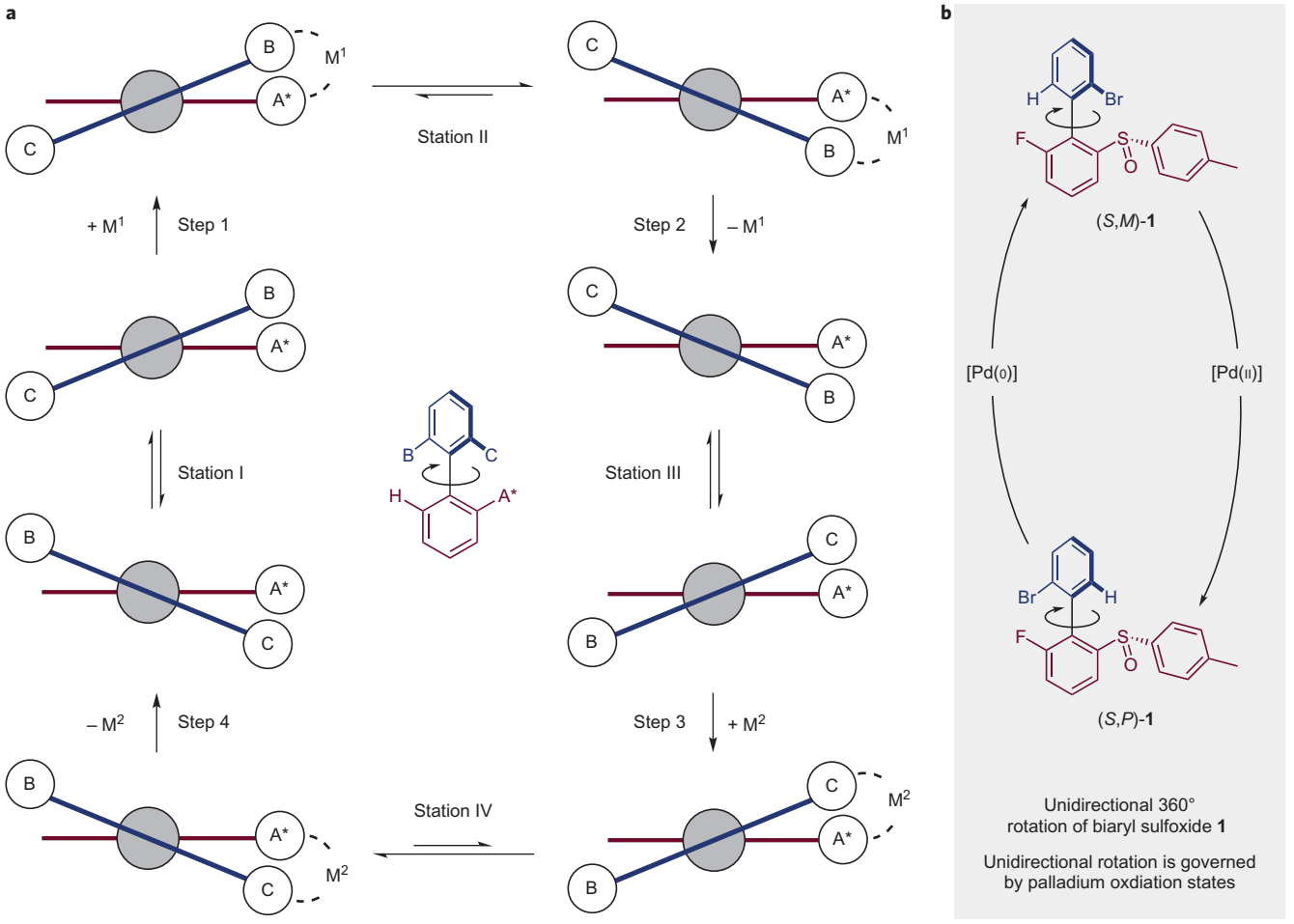

Figure 1 | Concept and design of a unidirectional rotary molecular motor. a, Blueprint for a 360° unidirectional rotary molecular motor. The upper aryl ring (the 'rotor', blue) rotates through 360° in a clockwise sense with respect to the lower aryl ring (the 'stator', red). Unidirectional rotation is governed by selective binding of a metal centre and the formation of diastereomeric metal complexes. **b**, Proposed realization of this system through the combination of biaryl sulfoxide **1** featuring axial and central chirality and a simple palladium salt allowing shuttling between Pd(0) and Pd(II) redox states.

transition-metal catalysis, we postulate that M^1 and M^2, rather than being different metals, could be two different oxidation states of the same transition metal. We envision a system that relies on the fundamental reactivity modes of organometallic chemistry: oxidative addition, ligand exchange, C–H activation and reductive elimination. The cycle depicted in Fig. 1a now describes the intersection of two unidirectional cycles: the physical rotation of one aryl group with respect to another and the cycle of transition-metal oxidation states. Here, we describe our studies towards the realization of such a system, with the combination of biaryl sulfoxide **1** and simple palladium salts (Fig. 1b), and report the first unidirectional molecular motor involving a single-bond rotary axle, governed by a cycle of transition-metal oxidation states.

Results and discussion

Our design for a unidirectional molecular motor is based on biaryl **1**, which exists as two atropisomers, (*S*,*M*)-**1** and (*S*,*P*)-**1**, where *S* denotes the fixed central chirality at sulfur, and *M* and *P* denote the chirality over the biaryl axis (Fig. 2; see Supplementary Sections 1–3 for the synthesis and full structural characterization of (*S*,*M*)-**1** and (*S*,*P*)-**1** and assignment of the axial chirality and absolute configuration of both isomers by single-crystal X-ray diffraction). Biaryl **1** draws on the biaryl sulfoxides investigated by Colobert, Wencel-Delord and co-workers[22,23], and we take advantage of the binding properties of the sulfoxide towards metal centres[24], the high thermal stability of the sulfoxide towards epimerization, and the proximity of the central chirality at sulfur to the axis of the biaryl[25,26]. The two atropisomers are conformationally stable with respect to the biaryl axis under ambient conditions, and density functional theory (DFT) calculations indicate a high barrier to atropisomerization and a small ground-state preference for (*S*,*P*)-**1** over (*S*,*M*)-**1** ($\Delta^{\ddagger}G° = 155$ kJ mol^{-1} and $\Delta G° = 3.5$ kJ mol^{-1}, respectively, see Supplementary Section 11 for full computational details).

In the first step of the 360° unidirectional rotation we envisioned that (*S*,*M*)-**1** could be transformed selectively into (*S*,*P*)-**1** via simple chemical manipulations, proceeding through a clockwise rotary motion of the upper aryl ring with respect to the lower ring, as shown in Fig. 2. Treatment of (*S*,*M*)-**1** with a palladium(II) complex might lead to selective reaction of the palladium centre with the *ortho* C–H bond of the upper aryl ring in a C–H activation event[27], forming palladacycle Pd[(*R*,*P*)-**2**]XL, where X and L are anionic and neutral ligands, respectively (note that neither the absolute helical nor point chirality have changed, but the stereochemical descriptors change due to palladium taking precedence on sulfur and over bromine). This process is underpinned by two key reactivity principles: (1) the sulfoxide acts as a directing group, bringing the palladium centre into close proximity with the *ortho* C–H bond via a six-membered ring, providing selective palladation; and (2) the inherent reactivity of the palladium(II) centre ensures its reaction with the C–H and not the C–Br bond.

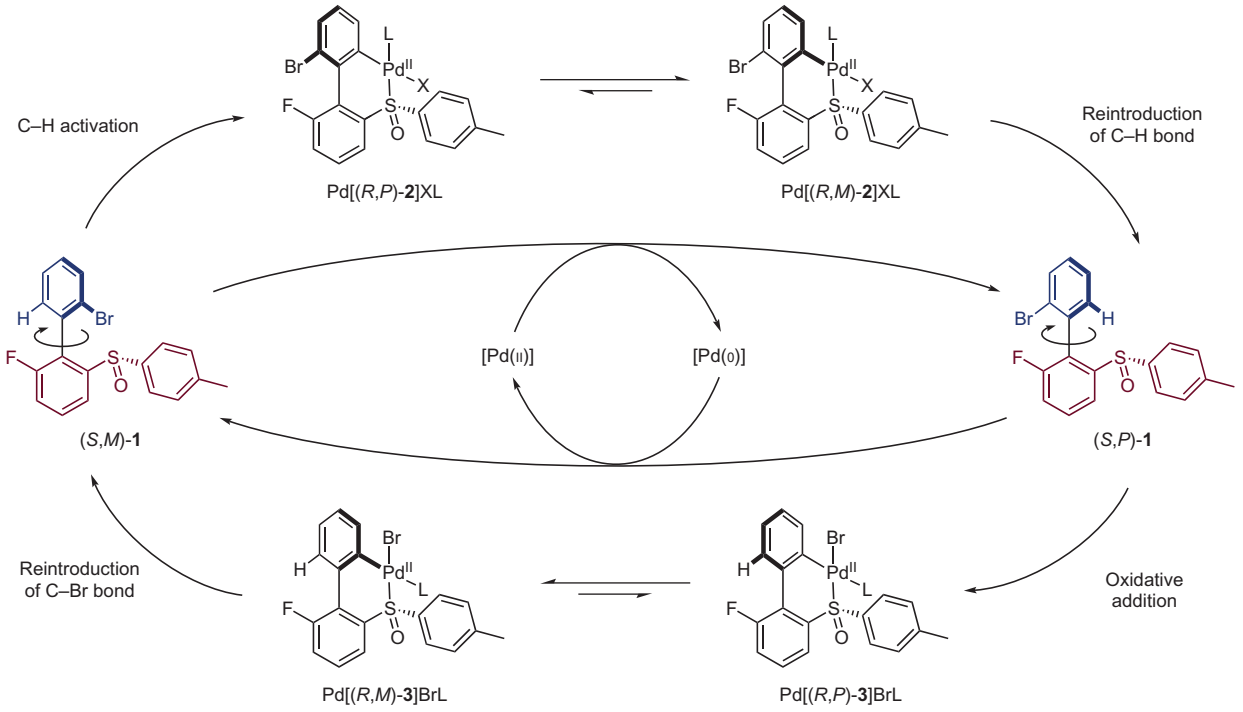

Figure 2 | Palladium-mediated 360° unidirectional rotation of biaryl 1. The upper aryl ring (the 'rotor', blue) rotates through 360° in a clockwise sense with respect to the lower aryl ring (the 'stator', red). Four key steps mediate the rotation: (i) C–H activation; (ii) reintroduction of the C–H bond; (iii) oxidative addition; and (iv) reintroduction of the C–Br bond.

Although (*S*,*M*)-**1** is 'locked' in the *M* axial configuration by the steric restrictions imposed by the *ortho* substituents, on formation of Pd[(*R*,*P*)-**2**]XL the barrier to atropisomerization is greatly reduced and the biaryl axis becomes configurationally labile, allowing the interconversion of Pd[(*R*,*P*)-**2**]XL and Pd[(*R*,*M*)-**2**]XL. Furthermore, these two diastereomeric palladacycles show a considerable energy difference; based on DFT calculations, Pd[(*R*,*M*)-**2**]XL has been shown to be lower in energy than the diastereomeric Pd[(*R*,*P*)-**2**]XL by 15.0 kJ mol^{-1} in a related model system (Supplementary Section 11). This energy difference would lead to a shifting of the atropisomerization equilibrium in favour of Pd[(*R*,*M*)-**2**]XL, facilitating a clockwise rotation across the biaryl axis. Subsequent transformation of the Pd–C bond in Pd[(*R*,*M*)-**2**]XL into a C–H bond would then provide (*S*,*P*)-**1**, completing a unidirectional clockwise 180° rotation.

The last decade has witnessed intense research interest into the use of C–H activation in chemical synthesis, but the transformation of (*S*,*M*)-**1** into (*S*,*P*)-**1** along this pathway would be the first use of C–H activation to control motion at the molecular level. Drawing on the orthogonal reactivity of palladium oxidation states, treatment of (*S*,*P*)-**1** with a palladium(0) source would also facilitate a clockwise 180° rotation: the palladium(0) complex will react with the C–Br bond via an oxidative addition reaction and the C–H bond will be left untouched. This leads to the formation of a new palladacycle Pd[(*R*,*P*)-**3**]BrL, in which we expect the coordination of the sulfoxide to the palladium(II) centre to form a six-membered bridge between the upper and lower aryl rings. Again, as for Pd[(*R*,*P*)-**2**]XL, the biaryl axis becomes conformationally labile and the barrier to atropisomerization for Pd[(*R*,*P*)-**3**]BrL and Pd[(*R*,*M*)-**3**]BrL is lowered (a barrier of 82.9 kJ mol^{-1} for the axial inversion has been calculated for related palladacycles, Supplementary Section 11). These diastereomeric palladacycles, again, have considerably different energies, and the equilibrium is shifted to Pd[(*R*,*M*)-**3**]BrL. From Pd[(*R*,*M*)-**3**]BrL, reintroduction of the Br–C bond completes the second 180° unidirectional rotation, delivering (*S*,*M*)-**1**. Closer analysis of the cycle described in Fig. 2 shows that the physical clockwise rotation of the upper aryl ring is coincident with a cycle through the palladium oxidation states from +2 to 0 to +2, that is, a catalytic redox cycle of the palladium atom. Although the whole system is not autonomous (due to the need for the addition of two sequential fuels to trigger the changes in oxidation state at the palladium centre), the rotary motor exhibits autonomous directionality: driven by the orthogonal reactivity of the palladium oxidation states, the motor itself determines the direction of rotation.

Subjecting diastereomerically pure (*S*,*M*)-**1** (>98%) to C–H activation conditions (Fig. 3, 1.5 equiv. of palladium acetate, 2 equiv. of trifluoroacetic acid and heating to 80 °C), followed by ligand exchange through treatment with lithium chloride in acetone provided a yellow solid. Based on its poor solubility in a number of common organic solvents and broad ^{1}H NMR spectra observed in *d*-chloroform, we postulate that this species is a mixture of the palladacycle dimer {Pd[(*R*,*M*)-**2**]Cl}$_2$ and related complexes with bridging [PdCl$_2$] units, which we denote {{Pd[(*R*,*M*)-**2**]Cl}$_2$ + [PdCl$_2$]$_x$}. These species are formed via axial inversion of the atropdiastereomeric {{Pd[(*R*,*P*)-**2**]Cl}$_2$ + [PdCl$_2$]$_x$}. The unidirectionality of the transformation of (*S*,*M*)-**1** into (*S*,*P*)-**1** was confirmed by characterization of the monomeric derivative C$_5$D$_5$N–Pd[(*R*,*M*)-**2**]Cl by one- and two-dimensional NMR spectroscopy experiments and high-resolution mass spectrometry (Fig. 3; see Supplementary Section 5 for further details; the axial helicity in C$_5$D$_5$N–Pd[(*R*,*M*)-**2**]Cl is assigned as *M* by subsequent reactivity and comparison with calculations of a related system).

To complete the 180° unidirectional rotation (that is, the conversion of (*S*,*M*)-**1** into (*S*,*P*)-**1**) the C–Pd bond in Pd[(*R*,*M*)-**2**]XL was transformed into a C–H bond (Fig. 3a). This could be accomplished via reductive elimination from an organopalladium(II) hydrido complex H–Pd[(*R*,*M*)-**2**]L with concomitant formation of a palladium(0) species. This hydride transfer–reductive elimination sequence could be accomplished, with complete stereoselectivity for the formation of (*S*,*P*)-**1** over (*S*,*M*)-**1** (>98%), through the treatment of {{Pd[(*R*,*M*)-**2**]Cl}$_2$ + [PdCl$_2$]$_x$} with the mild hydride

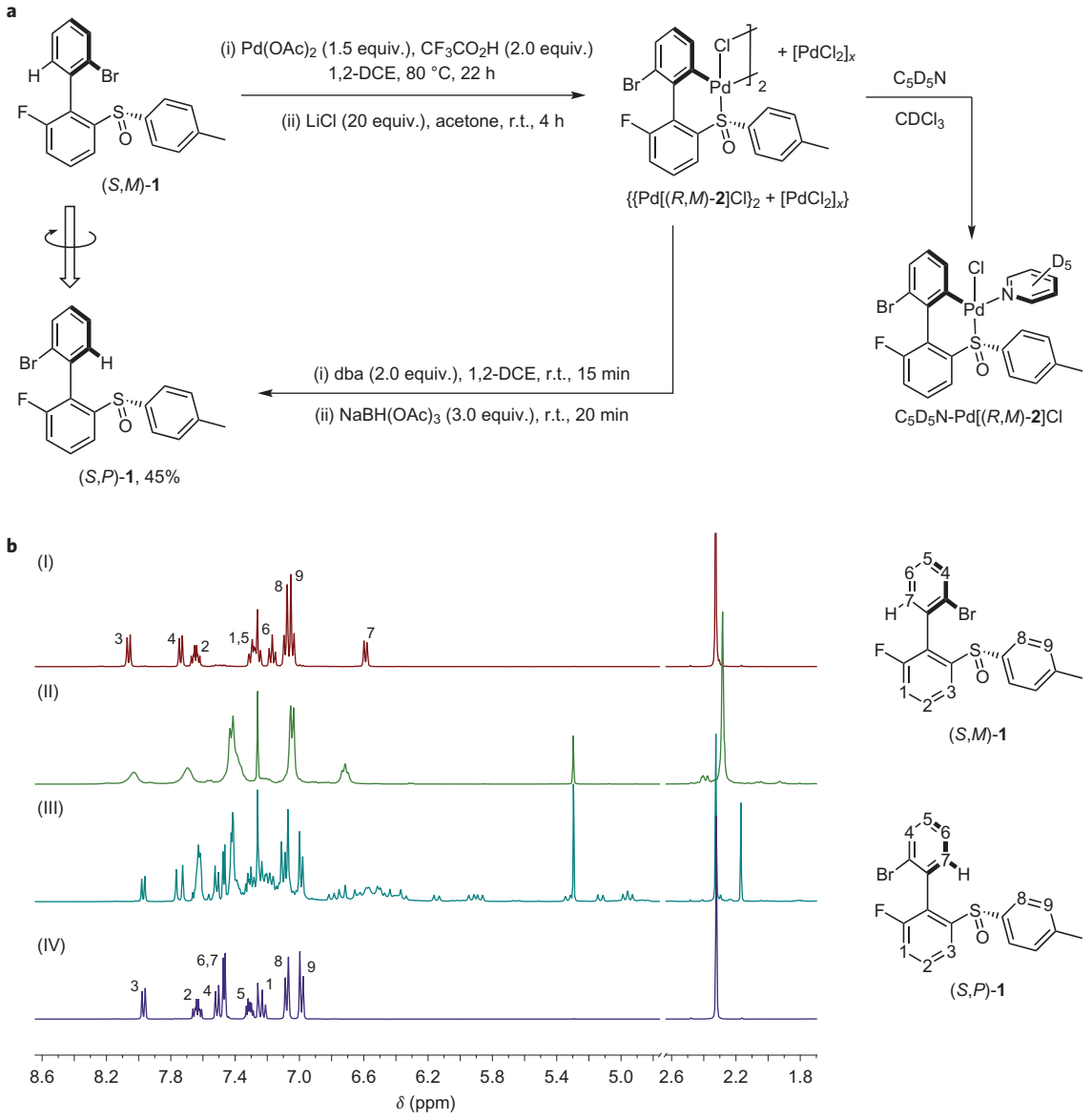

Figure 3 | Unidirectional 180° rotation of (*S*,*M*)-1 into (*S*,*P*)-1. a, Chemical structures and reaction scheme for unidirectional 180° rotation of (*S*,*M*)-**1** into (*S*,*P*)-**1**. The transformation of (*S*,*M*)-**1** into (*S*,*P*)-**1** follows a three-step protocol: (i) (*S*,*M*)-**1** was treated with $Pd(OAc)_2$ (1.5 equiv.) and CF_3CO_2H (2.0 equiv.) in 1,2-dichloroethane (1,2-DCE) at 80 °C for 22 h; (ii) ligand exchange via treatment with LiCl (20 equiv.) in acetone; (iii) the chloro-bridged palladium complex $\{\{Pd[(R,M)\text{-}\mathbf{2}]Cl\}_2 + [PdCl_2]_x\}$ was treated sequentially with *trans*,*trans*-dibenzylideneacetone (dba, ~2.0 equiv. with respect to the monomeric unit of $\{\{Pd[(R,M)\text{-}\mathbf{2}]Cl\}_2 + [PdCl_2]_x\}$) and sodium triacetoxyborohydride (~3.0 equiv. with respect to the monomeric unit of $\{\{Pd[(R,M)\text{-}\mathbf{2}]Cl\}_2 + [PdCl_2]_x\}$) in 1,2-DCE at room temperature; the structure of $\{\{Pd[(R,M)\text{-}\mathbf{2}]Cl\}_2 + [PdCl_2]_x\}$ was assigned based on full characterization of the corresponding d_5-pyridine adduct $C_5D_5N\text{-}Pd[(R,M)\text{-}\mathbf{2}]Cl$ (Supplementary Section 5). **b**, ^1H NMR spectra ($CDCl_3$, 400 MHz) of key intermediates in the transformation of (*S*,*M*)-**1** into (*S*,*P*)-**1**: (I) (*S*,*M*)-**1**; (II) $\{\{Pd[(R,M)\text{-}\mathbf{2}]Cl\}_2 + [PdCl_2]_x\}$; (III) crude reaction mixture following reduction of $\{\{Pd[(R,M)\text{-}\mathbf{2}]Cl\}_2 + [PdCl_2]_x\}$ with sodium triacetoxyborohydride (3.0 equiv.) in the presence of dba (2.0 equiv.); and (IV) (*S*,*P*)-**1**.

reducing agent sodium triacetoxyborohydride (STAB). Although direct treatment of $\{\{Pd[(R,M)\text{-}\mathbf{2}]Cl\}_2 + [PdCl_2]_x\}$ with STAB at room temperature did provide excellent selectivity for the formation of (*S*,*P*)-**1** over (*S*,*M*)-**1**, significant quantities of the over-reduced di-hydro species (*S*)-**4** were observed (see Supplementary Section 9 for further details). We reasoned that (*S*)-**4** was formed due to the presence of highly reactive ligandless palladium(0) species after the hydride reduction of the C–Pd bond in $\{\{Pd[(R,M)\text{-}\mathbf{2}]Cl\}_2 + [PdCl_2]_x\}$ and postulated that the introduction of stabilizing ligands would reduce the reactivity of the palladium(0) species towards direct reduction of the C–Br bond. Gratifyingly, treatment of $\{\{Pd[(R,M)\text{-}\mathbf{2}]Cl\}_2 + [PdCl_2]_x\}$ with 2 equiv. of *trans*,*trans*-dibenzylideneacetone (dba, a ligand known to support palladium(0) centres) before the addition of STAB limited the formation of (*S*)-**4**. ^1H NMR spectroscopy of the crude reaction mixture indicates that the palladium(0) species formed after this sequence is of the form Pd_2dba_3 (ref. 28). Thus, as depicted in Fig. 3, a 180° unidirectional rotation of (*S*,*M*)-**1** into (*S*,*P*)-**1** can be achieved in 45% overall yield through a C–H activation–ligand exchange–hydride transfer–reductive elimination sequence.

The unidirectional transformation of (*S*,*P*)-**1** into (*S*,*M*)-**1** was achieved as detailed in Fig. 4: a solution of (*S*,*P*)-**1** in tetrahydrofuran was treated with bis(dibenzylideneacetone)palladium(0) (0.75 equiv.) and tricyclohexylphosphine (2 equiv.) and heated to 40 °C overnight. Analysis of the reaction mixture by ^{19}F NMR spectroscopy showed the formation of a broad signal at −118.5 ppm

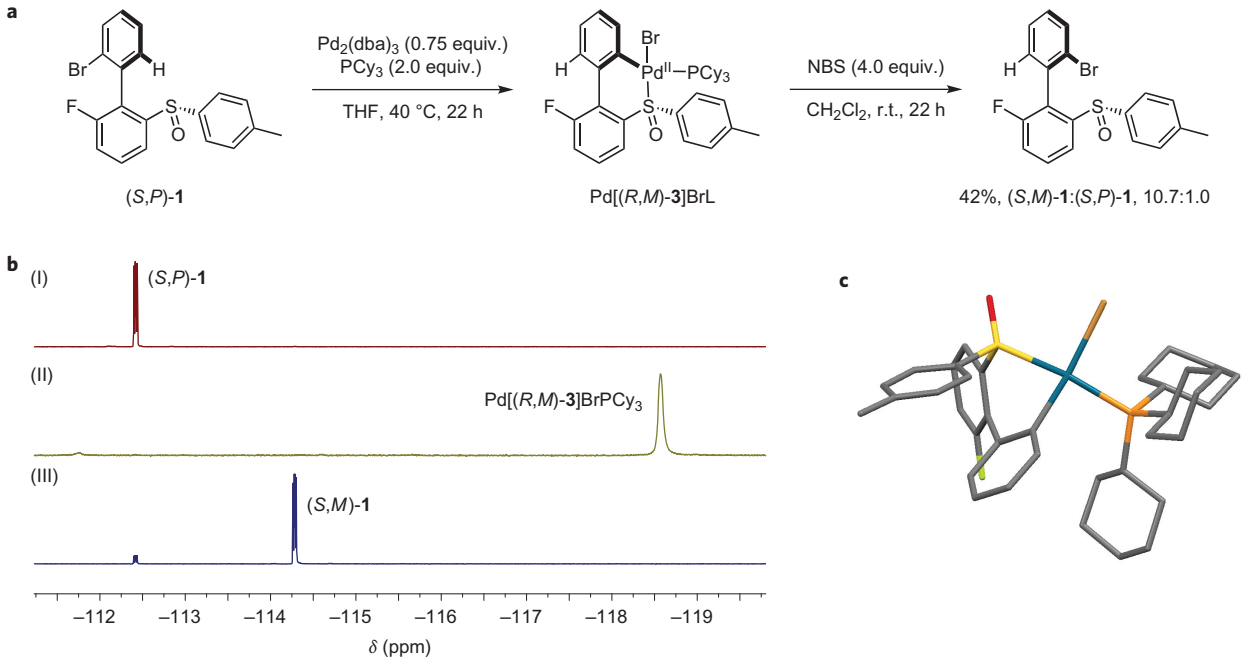

Figure 4 | Unidirectional 180° rotation of (*S*,*P*)-1 into (*S*,*M*)-1. a, Chemical structures and reaction scheme for unidirectional 180° rotation of (*S*,*P*)-**1** into (*S*,*M*)-**1**. (*S*,*P*)-**1** was treated with bis(dibenzylideneacetone)palladium(0) (Pd_2dba_3, 0.75 equiv.) and tricyclohexylphosphine (PCy_3, 2.0 equiv.) and heated to 40 °C in tetrahydrofuran (THF) for 22 h, followed by flash column chromatography to isolate Pd[(*R*,*M*)-**3**]BrPCy_3 and treatment with NBS (4.0 equiv.) to provide (*S*,*M*)-**1** in 42% yield, (*S*,*M*)-**1**:(*S*,*P*)-**1** = 10.7:1.0. **b**, ^{19}F NMR spectra ($CDCl_3$, 400 MHz) of key intermediates in the transformation of (*S*,*P*)-**1** into (*S*,*M*)-**1**: (I) (*S*,*P*)-**1**; (II) Pd[(*R*,*M*)-**3**]BrPCy_3; and (III) mixture of (*S*,*M*)-**1** and (*S*,*P*)-**1** obtained following treatment of Pd[(*R*,*M*)-**3**]BrPCy_3 with NBS (4.0 emsp14;equiv.) at room temperature and purification by flash column chromatography. **c**, The diastereomeric relationship between the central chirality at sulfur and the axial chirality was confirmed by the isolation and structural characterization by single X-ray diffraction of (±)-Pd[(*R*,*M*)-**3**]BrPCy_3.

that could be assigned to the desired oxidative addition complex Pd[(*R*,*M*)-**3**]BrPCy_3. Next, Pd[(*R*,*M*)-**3**]BrPCy_3 was subjected to standard bromination conditions (4 equiv. *N*-bromosuccinimide in dichloromethane at room temperature) to provide (*S*,*M*)-**1** in 42% yield in excellent selectivity ((*S*,*M*)-**1**:(*S*,*P*)-**1** of 10.7:1.00 by ^{19}F NMR) over the two steps. In a separate experiment, the clockwise pathway for the formation of (*S*,*M*)-**1** from (*S*,*P*)-**1** was confirmed by the isolation of Pd[(*R*,*M*)-**3**]BrPCy_3 and its full structural characterization by NMR, mass spectrometry and single-crystal X-ray diffraction (Fig. 4c), where the diastereomeric relationship between the central chirality at the sulfoxide and the chirality over the biaryl axis is clearly evident. Interestingly, the X-ray structure determination indicated the crystal to be racemic: the diffraction data were consistent with a centrosymmetric spacegroup. We attribute this to the fact that a mixture of (*S*,*P*)-**1** and (*S*,*M*)-**1** (1.0:3.2 by ^{19}F NMR) with slightly diminished enantiomeric excess (approximately <90%; see Supplementary Section 7 for further details) was used in the oxidative addition reaction (the racemate apparently crystallizes from solution).

Figures 3 and 4 describe two 180° unidirectional rotations, where the unidirectional rotation is derived from the inherent orthogonal reactivity of the two palladium oxidation states, the lowering of the barrier to rotation via the formation of a bridging palladacycle, and the transfer of chirality across the palladium atom from the sulfur point chirality to the biaryl axis. However, there is a further aspect of organopalladium chemistry that we have yet to harness: its catalytic capabilities. During the transformation of (*S*,*M*)-**1** into (*S*,*P*)-**1** (Fig. 3) a palladium(II) complex is converted into a palladium(0) species. As shown in Fig. 4, (*S*,*P*)-**1** reacts with a palladium(0) complex to provide (*S*,*M*)-**1** and what is likely to be the concomitant formation of palladium(II). As biaryl **1** undergoes a 360° physical rotation, the palladium atom undergoes a cycle of its oxidation states from palladium(II) to palladium(0) and back to palladium(II). Through careful choice of experimental conditions we hypothesized the development of a system based on two interconnected cycles: a physical rotation that is governed by a cycle of palladium oxidation states.

The realization of these interconnected cycles in a system with full rotary motion is shown in Fig. 5. As before, (*S*,*M*)-**1** was converted into (*S*,*P*)-**1** following C–H activation with palladium(II) acetate, hydride transfer from sodium triacetoxyborohydride and C–H reductive elimination (*vide supra*). Rather than subject this reaction mixture to purification (Fig. 3), we postulated that simple addition of tricyclohexylphosphine and a slight increase in temperature would be sufficient to activate the *in situ*-formed palladium(0) complexes towards oxidative addition into the C–Br bond of (*S*,*P*)-**1**. To our delight, addition of 1.5 equiv. of tricyclohexylphosphine and heating to 40 °C led to conversion of (*S*,*P*)-**1** to the oxidative addition complex Pd[(*R*,*M*)-**3**]BrPCy_3, as determined by the formation of a broad signal at –118.5 ppm in the ^{19}F NMR spectrum (Supplementary Section 7). Although the conversion is incomplete and some (*S*,*P*)-**1** remains (see Supplementary Section 8 for full details), subsequent bromination leads to the isolation of (*S*,*M*)-**1** and (*S*,*P*)-**1** in a 1.00:1.32 ratio in 45% yield (Fig. 5), where this ratio supports the transformation of Pd[(*R*,*M*)-**3**]BrPCy_3 into (*S*,*M*)-**1** in high selectivities, similar to those observed in Fig. 4. This experiment illustrates a unidirectional 360° rotation about a single bond driven by sodium triacetoxyborohydride and *N*-bromosuccinimide as chemical fuels in 19% overall yield, and proof of principle of a molecular rotary motor based on a palladium redox cycle. In principle, as a palladium(II) species is formed in the final step of the sequence, the system should be primed for spontaneous C–H activation and repetition of the rotary cycles following small adjustments to the reaction conditions. In practice, we expect that the presence of the electron-rich phosphine (tricyclohexylphosphine) in the reaction mixture will preclude subsequent C–H activation, and that further experimental optimization, in particular

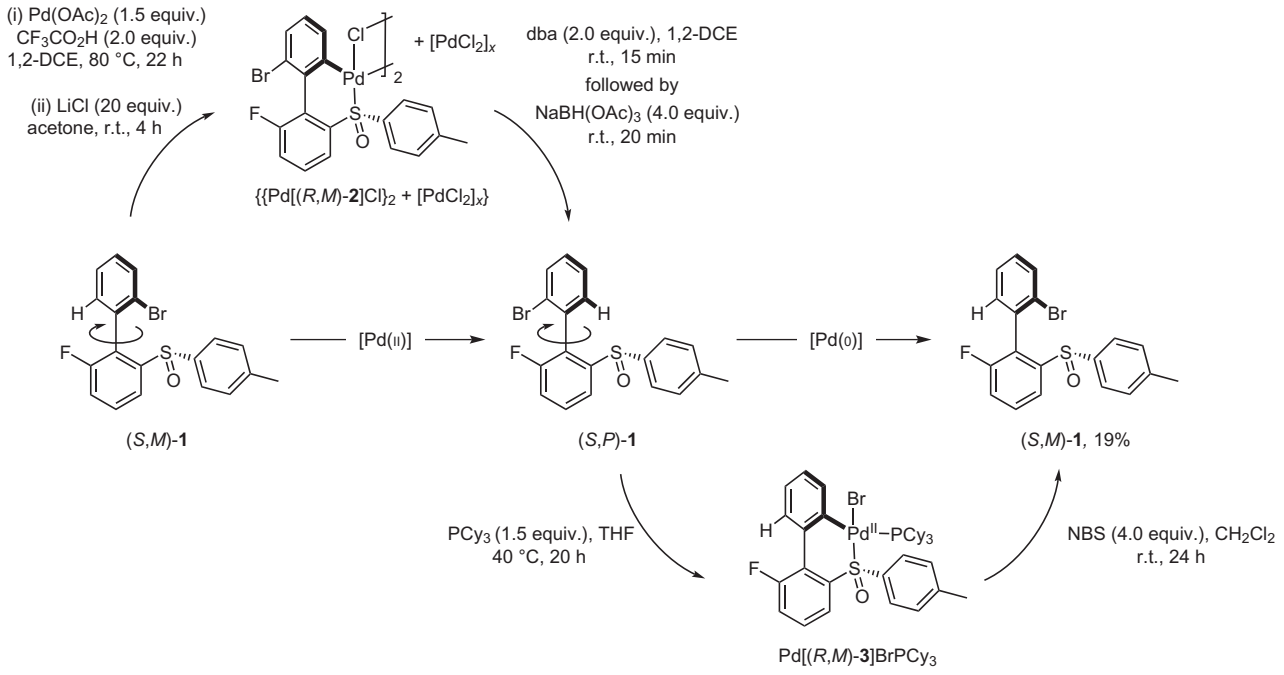

Figure 5 | Chemical structures and reaction scheme for an integrated cycle based on switching palladium(II) and palladium(0) redox states for unidirectional 360° rotation of (*S*,*M*)-1 into (*S*,*P*)-1 into (*S*,*M*)-1. Conditions mimic those described in Figs 3 and 4, except that following reduction with sodium triacetoxyborohydride, the reaction mixture was treated directly with tricyclohexylphosphine (PCy_3, ~1.5 equiv. with respect to the monomeric unit of {{Pd[(*R*,*M*)-**2**]Cl}$_2$ + [$PdCl_2$]$_x$}) and heated to 40 °C for 20 h. The reaction mixture was then treated with NBS (~4.0 equiv. with respect to the monomeric unit of {{Pd[(*R*,*M*)-**2**]Cl}$_2$ + [$PdCl_2$]$_x$}) at room temperature to provide a 1.00:1.32 mixture of (*S*,*M*)-**1** and (*S*,*P*)-**1** in 45% yield, representing a 19% overall yield obtained via a 360° rotational cycle.

modifying the ligands at palladium, is required to achieve multiple rotary cycles.

In conclusion, we have developed a molecular motor that undergoes 360° unidirectional rotation when combined with palladium and treated with chemical fuels. We envision that future studies will allow the development of a continuous organopalladium rotor through judicious choice of the reaction conditions and ligands. The feasibility of our molecular rotor is rooted in the reactivity principles that have underpinned the fields of organometallic chemistry and transition-metal catalysis over the past six decades: the orthogonal reactivity of different metal oxidation states, the unique steric environment offered to the ligands about transition-metal centres, which amplifies the communication between stereochemical elements, and the ease with which oxidation states can be cycled between and controlled by simple chemical reagents. It is interesting to note that the oxidation states of transition metals can be controlled not only with chemical reagents, but also through electrochemical methods. Future studies into the extension of the current system along these lines will provide fascinating prospects to realize an electrochemically powered molecular motor. Using powerful organometallic reactivity principles to control motion at the molecular scale represents an important advance in the development of complex molecular machines and takes us a major step towards the ultimate goal of the design of an autonomous continuously operating chemically fuelled catalytic molecular motor.

Received 9 March 2016; accepted 29 April 2016;
published online 6 June 2016

References

1. Champin, B., Mobian, P. & Sauvage, J.-P. Transition metal complexes as molecular machine prototypes. *Chem. Soc. Rev.* **36,** 358–366 (2007).
2. Coskun, A., Banaszak, M., Astumian, R. D., Stoddart, J. F. & Grzybowski, B. A. Great expectations: can artificial molecular machines deliver on their promise? *Chem. Soc. Rev.* **41,** 19–30 (2012).
3. Kay, E. R., Leigh, D. A. & Zerbetto, F. Synthetic molecular motors and mechanical machines. *Angew. Chem. Int. Ed.* **46,** 72–191 (2006).
4. Browne, W. R. & Feringa, B. L. Making molecular machines work. *Nature Nanotech.* **1,** 25–35 (2006).
5. Kinbara, K. & Aida, T. Toward intelligent molecular machines: directed motions of biological and artificial molecules and assemblies. *Chem. Rev.* **105,** 1377–1400 (2005).
6. Balzani, V., Credi, A. & Venturi, M. *Molecular Devices and Machines: Concepts and Perspectives for the Nanoworld* (Wiley, 2008).
7. Koumura, N., Zijlstra, R. W. J., van Delden, R. A., Harada, N. & Feringa, B. L. Light-driven monodirectional molecular rotor. *Nature* **401,** 152–155 (1999).
8. Koumura, N., Geertsema, E. M., van Gelder, M. B., Meetsma, A. & Feringa, B. L. Second generation light-driven molecular motors. Unidirectional rotation controlled by a single stereogenic centre with near-perfect photoequilibria and acceleration of the speed of rotation by structural modification. *J. Am. Chem. Soc.* **124,** 5037–5051 (2002).
9. Leigh, D. A., Wong, J. K. Y., Dehez, F. & Zerbetto, F. Unidirectional rotation in a mechanically interlocked molecular rotor. *Nature* **424,** 174–179 (2003).
10. Hernández, J. V., Kay, E. R. & Leigh, D. A. A reversible synthetic rotary molecular motor. *Science* **306,** 1532–1537 (2004).
11. Bissell, R. A., Córdova, E., Kaifer, A. E. & Stoddart, J. F. A chemically and electronically switchable molecular shuttle. *Nature* **369,** 133–137 (1994).
12. Ragazzon, G., Baroncini, M., Silvi, S., Venturi, M. & Credi, A. Light-powered autonomous and directional molecular motion of a dissipative self-assembling system. *Nature Nanotech.* **10,** 70–75 (2015).
13. Von Delius, M., Geertsema, E. M. & Leigh, D. A. A synthetic small molecule that can walk down a track. *Nature Chem.* **2,** 96–101 (2010).
14. Beves, J. E. *et al.* Toward metal complexes that can directionally walk along tracks: controlled stepping of a molecular biped with a palladium(II) foot. *J. Am. Chem. Soc.* **136,** 2094–2100 (2014).
15. Kelly, T. R., De Silva, H. & Silva, R. A. Unidirectional rotary motion in a molecular system. *Nature* **401,** 150–152 (1999).
16. Fletcher, S. P., Dumur, F., Pollard, M. M. & Feringa, B. L. A reversible unidirectional molecular rotary motor driven by chemical energy. *Science* **310,** 80–82 (2005).
17. Bringmann, G. & Hartung, T. First atropenantioselective ring opening of an achiral lactone-bridged biaryl with chiral borane-derived hydride-transfer reagents. *Angew. Chem. Int. Ed. Engl.* **31,** 761–762 (1992).
18. Bringmann, G. *et al.* Atropselective synthesis of axially chiral biaryl compounds. *Angew. Chem. Int. Ed.* **44,** 5384–5427 (2005).

19. Kakiuchi, F., Le Gendre, P., Yamada, A., Ohtaki, H. & Murai, S. Atropselective alkylation of biaryl compounds by means of transition metal-catalyzed C–H/olefin coupling. *Tetrahedron Asymmetr.* **11,** 2647–2651 (2000).
20. Ros, A. *et al*. Dynamic kinetic cross-coupling strategy for the asymmetric synthesis of axially chiral heterobiaryls. *J. Am. Chem. Soc*. **135,** 15730–15733 (2013).
21. Bhat, V., Wang, S., Stoltz, B. M. & Virgil, S. C. Asymmetric synthesis of QUINAP via dynamic kinetic resolution. *J. Am. Chem. Soc*. **135,** 16829–16832 (2013).
22. Hazra, C. K., Dherbassy, Q., Wencel-Delord, J. & Colobert, F. Synthesis of axially chiral biaryls through sulfoxide-directed asymmetric mild C–H activation and dynamic kinetic resolution. *Angew. Chem. Int. Ed*. **53,** 13871–13875 (2014).
23. Leroux, F. R., Berthelot, A., Bonnafoux, L., Panossian, A. & Colobert, F. Transition-metal-free atropo-selective synthesis of biaryl compounds based on arynes. *Chem. Eur. J*. **18,** 14232–14236 (2012).
24. Trost, B. M. & Rao, M. Development of chiral sulfoxide ligands for asymmetric catalysis. *Angew. Chem. Int. Ed*. **54,** 5026–5043 (2015).
25. Clayden, J., Mitjans, D. & Youssef, L. H. Lithium–sulfoxide–lithium exchange for the asymmetric synthesis of atropisomers under thermodynamic control. *J. Am. Chem. Soc*. **124,** 5266–5267 (2002).
26. Clayden, J., Fletcher, S. P., Rowbottom, S. J. M. & Helliwell, M. Conformational preferences of a polar biaryl: a phase- and enantiomeric purity-dependent molecular hinge. *Org. Lett*. **11,** 2313–2316 (2009).
27. Lyons, T. W. & Sanford, M. S. Palladium-catalyzed ligand-directed C–H functionalization reactions. *Chem. Rev*. **110,** 1147–1169 (2010).
28. Zalesskiy, S. S. & Ananikov, V. P. $Pd_2(dba)_3$ as a precursor of soluble metal complexes and nanoparticles: determination of palladium active species for catalysis and synthesis. *Organometallics* **31,** 2302–2309 (2012).

Acknowledgements

This work was supported financially by the European Research Council (Advanced Investigator Grant no. 227897 to B.L.F.), The Netherlands Organization for Scientific Research (NWO-CW), funding from the Ministry of Education and Science (Gravitation programme 024.001.035) and The Royal Netherlands Academy of Arts and Sciences (KNAW).

Author contributions

B.S.L.C. and B.L.F. conceived the project. B.S.L.C. performed the experimental work. J.C.M.K. performed the computational chemistry. E.O. solved the crystal structures. B.S.L.C. and B.L.F. wrote the manuscript. All authors read and commented on the manuscript.

Additional information

Supplementary information and chemical compound information are available in the online version of the paper. Reprints and permissions information is available online at www.nature.com/reprints. Correspondence and requests for materials should be addressed to B.L.F.

Competing financial interests

The authors declare no competing financial interests.